Journal of Applied Polymer Science

Parameters Characterizing the Kinetics of the Nonisothermal Crystallization of Thermoplastic Starch/Poly(lactic acid) Composites as Determined by Differential Scanning Calorimetry

Sha Li,[1,2] Zhouyi Xiong,[1] Peng Fei,[1,2] Jie Cai,[1,2] Hanguo Xiong,[1,2] Jun Tan,[1,2] Yan Yu[3]

[1]College of Food Science and Technology, Huazhong Agricultural University, Wuhan 430070, China

[2]Research Institute of Comprehensive Utilization of Biomaterials, Huazhong Agricultural University, Wuhan 430070, China

[3]International Central for Bamboo and Rattan, Beijing100102, China

Correspondence to: H. Xiong (E-mail: xionghanguo@163.com)

ABSTRACT: To guide the use of thermoplastic starch (TPS)/poly(lactic acid) (PLA) composites, the nonisothermal crystallization kinetics of pure PLA and TPS/PLA composites were investigated with differential scanning calorimetry (DSC) at three different cooling rates. The results indicate that the TPS/PLA composites showed different crystallizations because of their different contents and different cooling rates. TPS, as a nucleating agent, improved the crystallinity of the PLA and constrained the mobility of the PLA chains. Three theoretical models, namely, the Avrami, Ozawa, and Mo models, were used to describe the process of nonisothermal crystallization. The Avrami analysis modified by Jeziorny and the Mo method was successful in describing the nonisothermal crystallization process of the pure PLA and the TPS/PLA composites. However, the Ozawa analysis could not give an adequate description. Kinetic parameters such as the Avrami exponent, kinetic crystallization rate constant, relative degree of crystallinity, and crystallization enthalpy, among others, were determined at various scanning rates. © 2013 Wiley Periodicals, Inc. J. Appl. Polym. Sci. 000: 000–000, 2013

KEYWORDS: biodegradable; composites; differential scanning calorimetry (DSC)

Received 31 May 2012; accepted 17 September 2012; published online
DOI: 10.1002/app.38587

INTRODUCTION

With the development of technology in petrochemical polymers, an increasing number of nondegradable materials have been introduced. However, the environment has also become considerably polluted and damaged as a result of the use of nondegradable materials for disposable items.[1–3] In recent years, the growing concern regarding environmental issues and the need for biodegradable materials have stimulated interest in biodegradable polymers.[4,5]

As an abundant raw material with low cost, starch has many distinguishing features and has been considered a dynamic source material.[6] It has been applied in the production of degradable plastics and blend films, which are materials used commonly in the agricultural, medicine, and packaging industries.[7] However, compared with most petroleum-based polymers, the poor mechanical properties and relatively high hydrophilic nature of starch prevent its widespread use in many applications. For improving the mechanical properties of the material, the blending of starch with other polymers is considered to be the simplest method.

Poly(lactic acid) (PLA) is the most widely used commercial polymer because of its superior biodegradability and mechanical properties.[8] However, its high cost and slow rate of degradation mainly hinder its application in many high-technology areas.[9,10] To address these problems, PLA is usually mixed with other cheap biodegradable polymers.[11] Blending is also commonly used to improve the properties of polymers.[12]

To overcome the aforementioned drawbacks of PLA and starch, PLA was mixed with starch. The miscible blending of starch with PLA was expected to improve their respective undesirable properties and exhibit a certain synergistic effect as well. For example, the addition of modified starch into PLA is advantageous in terms of reducing costs and preventing environmental pollution.[13] The melting temperature and onset temperature (T_{onset}) of the crystallization of the modified starch/PLA composites decreased with the addition of modified starch into PLA; this had a great significance for practical applications. Recently, some works on PLA and starch blends have also been published. Yew et al.[14] studied the effect of rice starch on the mechanical,

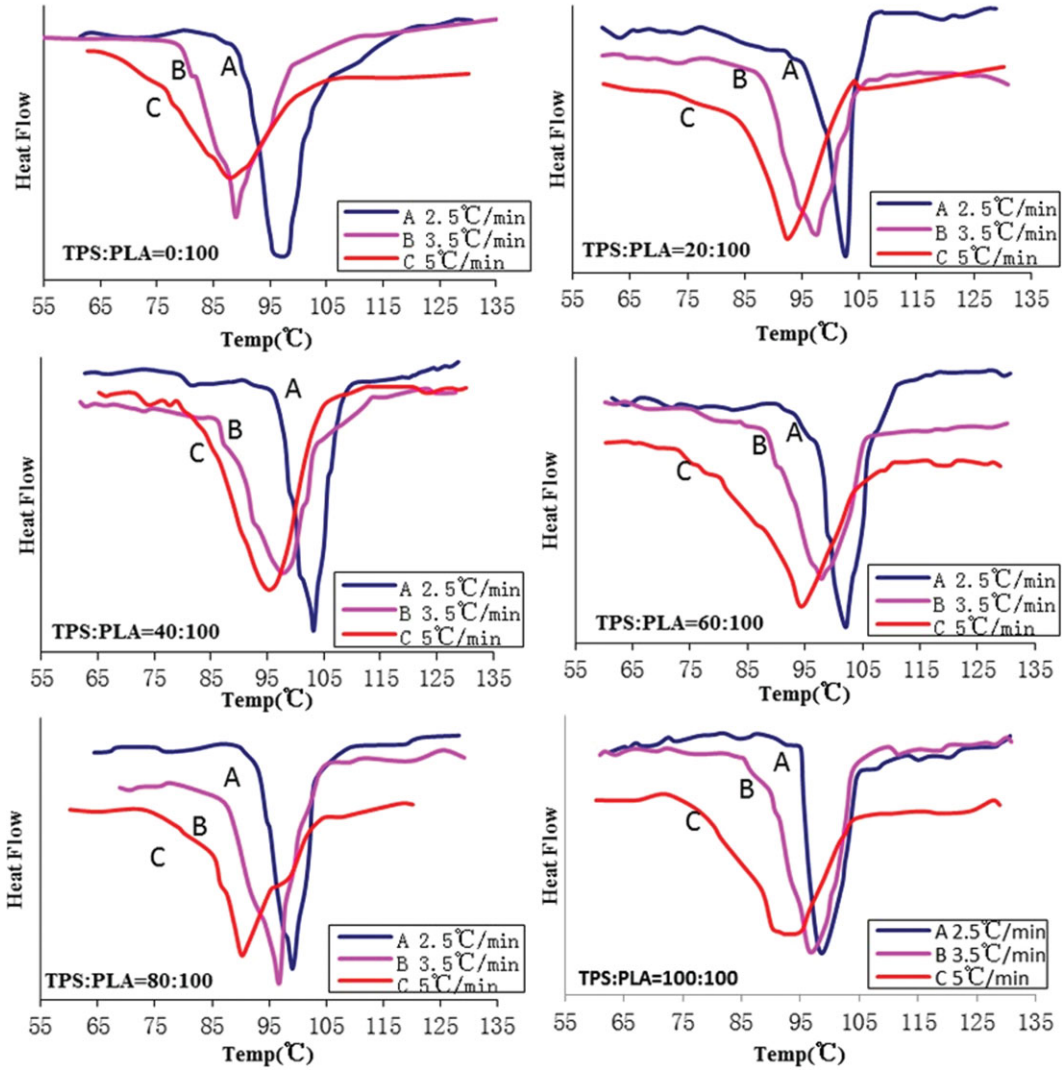

Figure 1. Nonisothermal crystallization exotherms of the samples at different φs. [Color figure can be viewed in the online issue, which is available at www.interscience.wiley.com.]

morphology, water absorption, and enzymatic degradation behaviors of PLA composites. Chanakorn and Rangrong[15] used three different types of amphiphilic molecules to produce thermoplastic starch (TPS)/PLA composites. However, there have been few recent studies on the nonisothermal crystallization kinetics of TPS/PLA composites.

The crystallization behavior of polymers is a basic problem in polymer physics. Particularly, the filler in the polymer substantially affects the crystallization behavior of polymer-based composites. The crystallization process can proceed under either isothermal or nonisothermal conditions. However, studies of the isothermal conditions are more common because of the easier theoretical treatment of the data. From a practical view, polymers and composites usually undergo nonisothermal crystallization processes in a practical process, so nonisothermal crystallization is more useful than the isothermal one. The investigation of the crystallization behavior can serve as a guide for processes and applications.[13] In this study, the crystallization behavior of pure PLA and TPS/PLA composites was observed with differential scanning calorimetry (DSC). The nonisothermal crystallization kinetics of the PLA and TPS/PLA composites were also examined.

EXPERIMENTAL

Materials

PLA pellets were acquired from NatureWorks with a number-average molecular weight of 1.4×10^4 g/mol and were dried in an air oven at 80°C for 5 h before use. Meanwhile, corn starch was provided by the Research Institute of Comprehensive Utilization of Biomaterials, Huazhong Agricultural University (Wuhan, China). The starch was dried at 100°C for 5 h to ensure that no weight loss occurred. The glycerol was produced by China National Pharmaceutical Group and had a boiling point of 563 K (101.3KPa). The starch was modified by glycerol as a plasticizer (10 : 3 starch/glycerol w/w) to obtain TPS before use. The starch and glycerol were mixed by a stirring kneader (NH-20 Rugao Tong-da Machinery Manufacturing, China) at 80°C for 10 min.

Table I. T_{onset}, T_{peak}, $t_{1/2}$, ΔH, n, and Z_c Values at Different φs

Sample	φ (°C/min)	T_{onset} (°C)	T_{peak} (°C)	$T_{onset} - T_{peak}$ (°C)	ΔH (J/g)	$t_{1/2}$ (min)	n	Z_c
TPS/PLA	2.5	119.0	98.2	20.8	30.05	7.50	2.35	0.13
0 : 100	3.5	109.0	88.9	20.1	22.58	5.23	2.25	0.31
	5	108.0	87.6	20.4	13.75	4.47	2.28	0.47
TPS/PLA	2.5	109.1	102.7	6.4	40.10	3.06	1.85	0.38
20 : 100	3.5	110.9	97.7	13.2	31.60	4.32	2.56	0.31
	5	106.8	92.6	14.2	23.71	3.09	1.91	0.60
TPS/PLA	2.5	111.8	103.2	8.6	21.12	4.21	2.48	0.21
40 : 100	3.5	109.1	97.7	11.4	18.76	3.78	2.35	0.37
	5	110.7	95.2	15.5	16.36	3.68	3.07	0.42
TPS/PLA	2.5	109.2	101.9	7.3	15.89	3.26	2.20	0.31
60 : 100	3.5	108.4	97.8	10.6	14.11	3.25	2.25	0.42
	5	106.2	94.2	12.0	10.17	2.36	2.26	0.63
TPS/PLA	2.5	106.6	99.0	7.6	15.29	3.25	2.87	0.22
80 : 100	3.5	108.0	96.8	11.2	13.70	3.48	2.72	0.34
	5	104.1	90.2	13.9	9.46	2.84	2.80	0.52
TPS/PLA	2.5	107.6	98.7	8.9	14.76	3.02	2.70	0.26
100 : 100	3.5	105.8	96.7	9.1	12.13	2.57	2.57	0.45
	5	103.5	92.7	10.8	9.37	2.46	2.17	0.63

ΔH: crystallization enthalpy.

Preparation of the TPS/PLA Composites

The ratios of TPS to PLA particles were 0 : 100, 20 : 100, 40 : 100, 60 : 100, 80 : 100, and 100 : 100 w/w, respectively. The TPS and PLA were mixed by the stirring kneader at 175–180°C for 10–15 min. The resulting sheet was compression-molded at 180°C into a 1 mm thick sheet under a pressure of 9 MPa for 15 min and then kept at room temperature.

Thermal Measurements

Thermal analysis of the TPS/PLA composites was carried out with a Nexus DSC 204F1 instrument which is made from Freistaat Bayern of Germany in a nitrogen atmosphere. The DSC instrument was calibrated with the melting temperature and enthalpy of the standard material indium at each cooling rate (φ) in the measurement. Samples 5–10 mg were weighed accurately into an aluminum pan and sealed hermetically. An empty pan was used as a reference. The DSC temperature increased from 20 to 200°C above the melting temperature at a heating rate of 30°C/min and kept at this temperature for 5 min to eliminate the thermal history of samples. Then, the samples were cooled to 20°C at three different φs, 2.5, 3.5, and 5°C/min, respectively.

Theoretical Background

Avrami Method. One of the most common models used to describe overall isothermal crystallization kinetics is the Avrami model. On the basis of the simplified assumption that crystallization occurs under a constant temperature, the kinetic parameters of nonisothermal crystallization were determined. Therefore, the Avrami equation[16–18] can be used as follows:

$$1 - X_t = \exp(-Z_t t^n) \tag{1}$$

where X_t is the relative degree of crystallinity; n is the Avrami crystallization exponent, a dimensionless constant related to nucleation and growth mechanisms; Z_t is the crystallization rate constant; and t is the time taken during the crystallization process.

In Eq. (1), X_t is defined in the following equation:

$$X_t = \frac{\int_{T_0}^{T}(dH_c/dT)dT}{\int_{T_0}^{T_\infty}(dH_c/dT)dT} \in (0,1) \tag{2}$$

where dH_c/dT denotes the heat flow at temperature T and T_∞ and T_0 are the end and the onset crystallization temperature, respectively.

To handle the data conveniently, eq. (1) is usually written in a double-logarithmic form as follows:

$$\ln[-\ln(1 - X_t)] = \ln Z_t + n \ln t \tag{3}$$

Nonisothermal crystallization can also be analyzed with the Avrami equation, but considering the characterization of the investigated process, Jeziorny[19] considered the effect of φ. Therefore, Z_t was corrected by φ as follows:

$$\ln Z_c = (\ln Z_t)/\varphi \tag{4}$$

where Z_c is the kinetic crystallization rate constant.

Ozawa Method. Nonisothermal crystallization is a rate-dependent process, so Ozawa[20] took into account the effect of φ and extended the Avrami equation to describe the kinetics of nonisothermal crystallization. Compared with the Avrami model, the main difference was that the time variable was replaced by φ.

Applied Polymer SCIENCE

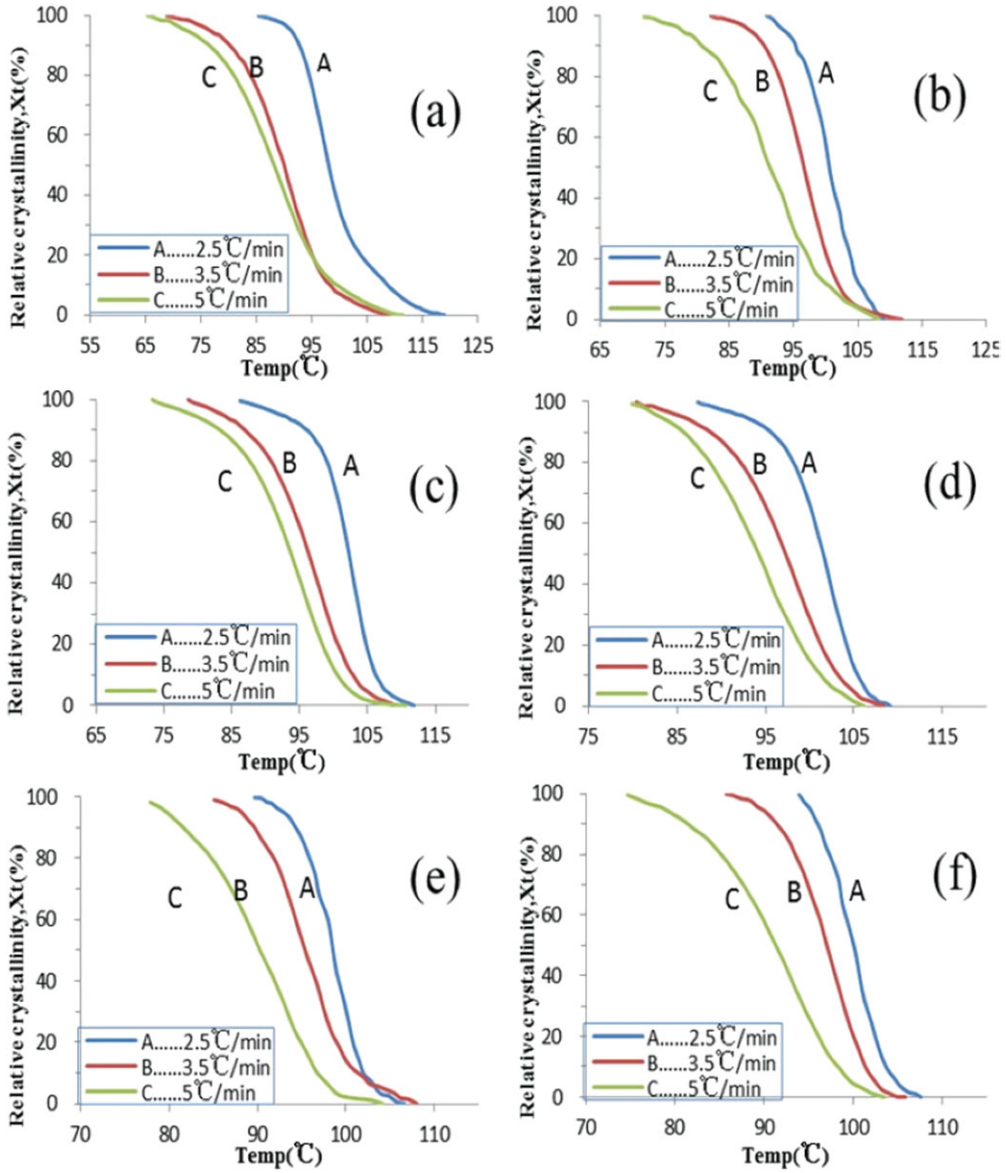

Figure 2. Plots of X_t versus t for the nonisothermal crystallization of the samples at three φs: (a) TPS/PLA = 0 : 100, (b) TPS/PLA = 20 : 100, (c) TPS/PLA = 40 : 100, (d) TPS/PLA = 60 : 100, (e) TPS/PLA = 80 : 100, and (f) TPS/PLA = 100 : 100 w/w. [Color figure can be viewed in the online issue, which is available at www.interscience.wiley.com.]

With the assumption that the nonisothermal crystallization process may be composed of infinitesimally small isothermal crystallization steps, the following equation was derived:

$$\ln[-\ln(1 - X_t) = \ln K(T) - m \ln \varphi] \tag{5}$$

where $K(T)$ is the crystallization rate constant and m is the Ozawa exponent, which depends on the nucleation mechanism and crystal growth.

Mo Method. Mo proposed a different kinetic equation to describe nonisothermal crystallization in which the Avrami equation was combined with the Ozawa equation. Its final form is given as follows:[21,22]

$$\ln \varphi = \ln F(T) - \alpha \ln t \tag{6}$$

where α refers to the ratio of n to the Ozawa exponent m ($\alpha = n/m$) and the parameter $F(T) = [K(T)/Z_t]^{1/m}$, where $F(T)$ refers to the value of the φ chosen at a certain crystallization time when the system amounts to a certain degree of crystallinity. The smaller the value of $F(T)$ was, the higher the crystallization rate became. Therefore, $F(T)$ has a definite physical and practical meaning.

RESULTS AND DISCUSSION

Nonisothermal Crystallization Behavior of the PLA and Starch/PLA Composites

The DSC curves of the pure PLA and TPS/PLA composites at three φs of 2.5, 3.5, and 5°C/min are shown in Figure 1. Some kinetic parameters can be derived from the nonisothermal crystallization exotherms, such as T_{onset}, which is the

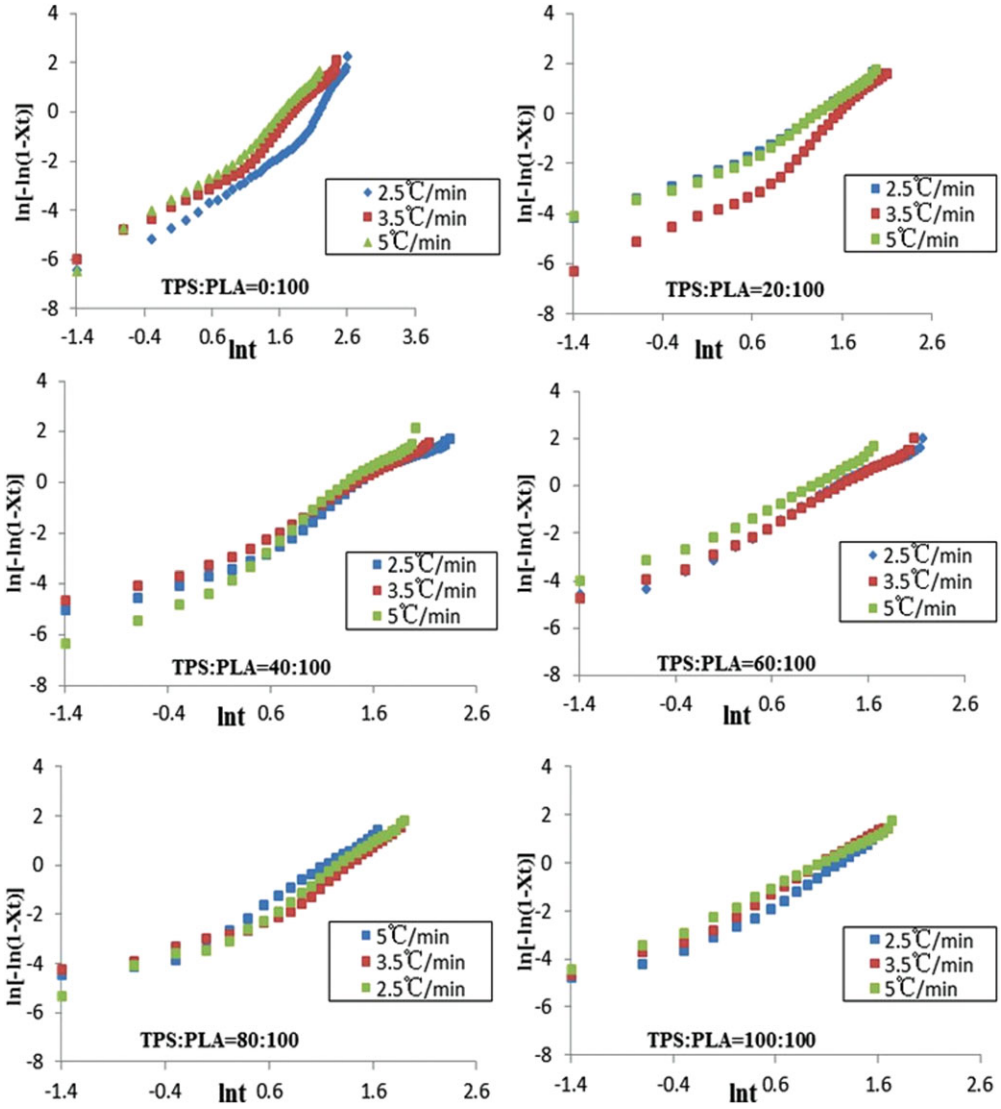

Figure 3. Plots of $\ln[-\ln(1 - X_t)]$ versus $\ln t$ for the nonisothermal crystallization of samples at three φs. [Color figure can be viewed in the online issue, which is available at www.interscience.wiley.com.]

temperature at the crossing point of the tangents of the baseline and the high-temperature side of the exotherm; the half-crystallization time ($t_{1/2}$), which is the time required for 50% crystallization; X_t, the crystallization enthalpy (ΔH_c); and the peak temperature (T_{peak}). The kinetic parameters are listed in Table I.

As shown in Table I, there was a decrease in T_{onset} and $t_{1/2}$ of pure PLA when φ increased, but there were no irregular changes in the same variables of the TPS/PLA composites after the addition of TPS into PLA. The range of T_{onset} of the composites was 100–110°C. However, the T_{peak} values of both the pure PLA and the TPS/PLA composites decreased when φ increased; that is, the faster φ was, the lower the temperature at which the maximum crystallization rate occurred. At the same time, for a given φ, T_{peak} of the TPS/PLA composites was slightly higher than that of the pure PLA; this indicated that the addition of TPS into PLA increased the crystallization rate of PLA. Furthermore, with an increase in φ, there was a larger range difference between T_{onset} and T_{peak}. At a slower φ, there was sufficient time for the activation of the nuclei at a higher temperature. On the contrary, at a faster φ, there was inadequate time for the activation of the nuclei. Therefore, the activation occurred at a lower temperature. $t_{1/2}$ also proved this finding.

As shown in Table I, ΔH_c decreased as φ increased, but it shifted to lower values when the TPS loading in the composites increased. Furthermore, for a given φ, ΔH_c of the TPS/PLA composites (TPS/PLA = 20 : 100) was higher than that of pure PLA, which indicated that TPS could act as a nucleating agent for PLA. However, when the ratio of TPS to PLA was higher than 0.2, ΔH_c of the TPS/PLA composites was lower than that of pure PLA. This finding indicated that with a decrease in the PLA content of the composite, ΔH_c also decreased. In addition, TPS hindered the activity of the PLA chains, which affected the crystallization of PLA during the crystallization process.

Applied Polymer SCIENCE

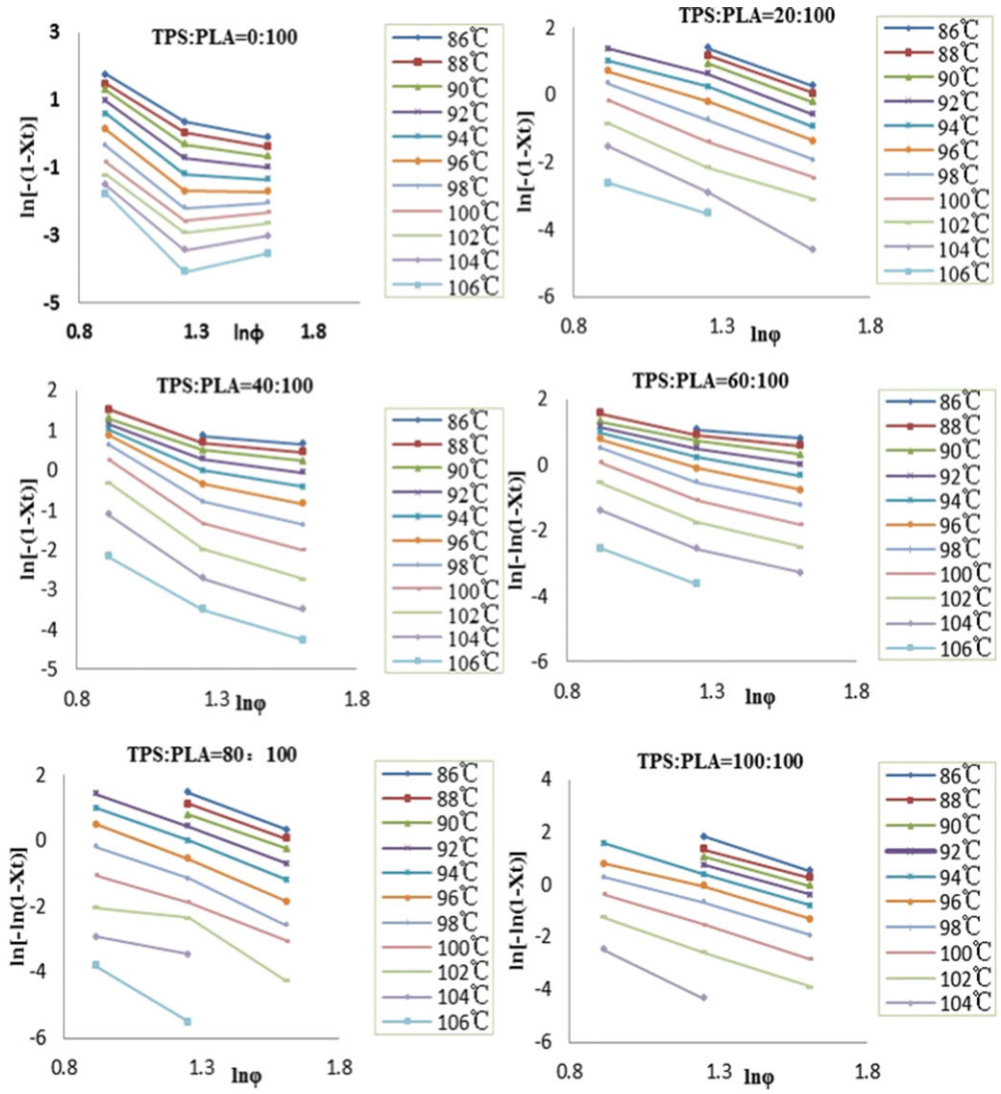

Figure 4. Plots of $\ln[-\ln(1 - X_t)]$ versus $\ln \varphi$ for the nonisothermal crystallization of the samples. [Color figure can be viewed in the online issue, which is available at www.interscience.wiley.com.]

X_t was obtained from the area of the exothermic peak of the nonisothermal crystallization analysis by DSC. X_t is a function of the temperature, as plotted in Figure 2. This figure shows that all of the curves had the same S shape. Because of the shorter crystallization time at a faster φ, the values of X_t were lower than those at a slower φ at the same crystallization temperature.

Nonisothermal Crystallization Kinetics of the TPS/PLA Composites

Avrami Method. From the plotting of $\ln[-\ln(1 - X_t)]$ versus $\ln t$ for the nonisothermal crystallization of the pure PLA and the TPS/PLA composites at each φ, straight lines were obtained. These are shown in Figure 3. From the slope and intercept of the lines, we determined n and Z_t, which are listed in Table I. The temperature varied constantly in nonisothermal crystallization, which affected the rates of spherulite growth and nuclei formation ascribed to their temperature dependence. Therefore, the Z_t and n parameters did not have the same physical meaning as in isothermal crystallization.

As shown in Table I, the range of n was 2–3; this indicated that the nonisothermal crystallization of the pure PLA and the TPS/PLA composites corresponded to a three-dimensional growth with homogeneous nucleation. The Z_c values of the TPS/PLA composites were also higher than that of the pure PLA for a given φ. This result indicates that the crystallization rates of the TPS/PLA composites were faster than that of the pure PLA; this also proved that TPS acted as a nucleating agent for PLA. In addition, with increasing φ, the value of Z_c increased for the pure PLA and the TPS/PLA composites. This finding indicated that the faster φ was, the faster the crystallization rate was.

Ozawa Method. In this approach, for a given temperature, the raw data were the relative crystallinity function of φs, such as those shown in Figure 4. Data analysis according to this method could be accomplished by a drawing of the plot of

Table II. Nonisothermal Crystallization Kinetic Parameters Based on the Mo Method

Sample	X_t	$F(T)$	α
TPS/PLA = 0 : 100	0.2	2.85	1.10
	0.4	3.01	1.03
	0.6	3.40	1.15
	0.8	4.02	1.37
TPS/PLA = 20 : 100	0.2	1.52	0.32
	0.4	1.85	0.53
	0.6	2.27	0.76
	0.8	3.13	1.21
TPS/PLA = 60 : 100	0.2	1.62	0.57
	0.4	1.88	0.69
	0.6	2.39	0.96
	0.8	2.88	1.16
TPS/PLA = 100 : 100	0.2	2.10	1.64
	0.4	2.95	2.02
	0.6	3.83	2.42
	0.8	5.45	3.23

$\ln[-\ln(1 - X_t)]$ versus $\ln \varphi$ at a given temperature, where the kinetic parameters m and $K(T)$ were derived from the slope and the intercept, respectively. The temperature range was 92–104°C for the cooling crystallization process.

As shown in Figure 4, the Ozawa equation did not describe the nonisothermal crystallization of the pure PLA and TPS/PLA composites well because of the nonlinear dependence of $\ln[-\ln(1 - X_t)]$ on $\ln \varphi$. For PLA and it composites, crystallization was complicated because of an additional slow process, which involved the improvement of the crystalline order and was referred to as *secondary crystallization*. The secondary crystallization effect for PLA may have been the reason for the nonsuitability of the Ozawa equation.

Mo Method. The $\ln \varphi$ was plotted versus $\ln t$ for the nonisothermal crystallization of the pure PLA and the TPS/PLA composites (0 : 100, 20 : 100, 60 : 100, and 100 : 100) at each relative crystallinity (X_t = 0.2, 0.4, 0.6, and 0.8). The data of the kinetic parameter $F(T)$ and α could be estimated from the intercept and slope, and these are shown in Table II.

α values increased as X_t increased, but the physical meaning of α was not clear. By comparing the values of $\ln F(T)$ of the different samples, we found the values of pure PLA to be larger than those of the TPS/PLA composites. This result indicated that the crystallization rate of the TPS/PLA composites was faster than that of pure PLA; this was in accordance with the results obtained from the Avrami model. In addition, for a given sample, the values of $\ln F(T)$ increased with increasing X_t. This finding implied that a higher φ should be used within the unit crystallization time at a given degree of crystallinity and indicated that the higher X_t is, the more difficult polymer crystallization is.

CONCLUSIONS

TPS/PLA composites prepared by melt compounding were investigated with DSC, and the results showed that there were different crystallizations at varied contents of TPS in the composites and at different φs. Moreover, the T_{peak} values of the TPS/PLA composites were slightly higher than that of pure PLA; this indicated that the addition of TPS into PLA increased the crystallization rate of PLA. ΔH_c of the TPS/PLA composite (TPS/PLA = 20 : 100) was also higher than that of pure PLA; this implied that TPS acted as a nucleating agent for PLA. However, when the ratio was higher than 0.2, ΔH_c of the composites was lower than that of pure PLA; this suggested that TPS hindered the activity of PLA chains and affected the crystallization of PLA during the crystallization process.

The nonisothermal crystallization kinetics of each sample were analyzed according to three kinetic models, namely, the Avrami, Ozawa, and Mo models. The Ozawa equation failed to provide an adequate description of the nonisothermal crystallization. Meanwhile, the Avrami equation modified by Jeziorny and the Mo method were successful in describing the nonisothermal crystallization process of the neat PLA and the TPS/PLA composites. In the Avrami method, the parameter Z_c suggested that the crystallization rates of all of the samples increased with increasing φ. TPS was also proven to act as a nucleating agent for PLA. The value of n showed that the nonisothermal crystallization of the pure PLA and the TPS/PLA composites corresponded to a three-dimensional growth with a homogeneous nucleation. These were consistent with the findings obtained from the Mo method.

ACKNOWLEDGMENT

The authors acknowledge the financial assistance provided for this work from National Science and Technology Support Program?contract grant number 2012BAD54G01), Huazhong Agricultural University Outstanding Graduate Student Innovation Research program (contract grant number 2012SC21), the National Natural Science Foundation of China (contract grant number 20976066) and the Fundamental Research Funds for the Central Universities (contract grant number 2011PY152).

REFERENCES

1. Suprakas, S. R.; Kazunobu, Y.; Masami, O.; Akinobu, O.; Kazue, U. *Chem. Mater.* **2003**, *15*, 1456.
2. Ke, T. Y.; Sun, X. Z. *Cereal Chem.* **2000**, *77*, 761.
3. Zou, P.; Tang, S. W.; Fu, Z. Z.; Xiong, H. G. *Int. J. Therm. Sci.* **2009**, *48*, 837.
4. Zainab, Z.; Pitt, S. *Polym. Test.* **2006**, *25*, 807.
5. Zhao, W. Y.; Andrzej, K.; James, E. *M. Chem. Mater.* **1998**, *10*, 794.
6. Vaidya, U. R.; Bhattacharya, M. *J. Appl. Polym. Sci.* **1994**, *52*, 617.

7. Xiong, H. G.; Tang, S. W.; Tang, H. L.; Zou, P. *Carbohydr. Polym.* **2008**, *71*, 263.
8. Juntuek, P.; Ruksakulpiwat, C.; Chumsamrong, P.; Ruksakulpiwat, Y. *J. Appl. Polym. Sci.* **2012**, *125*, 745.
9. Chen, H. P.; Marek, P.; Peggy, C. *Thermochim. Acta* **2009**, *492*, 61.
10. Sheth, M.; Kumar, R. A.; Dave, V.; Gross, R. A.; McCarthy, S. P. *J. Appl. Polym. Sci.* **1997**, *66*, 1495.
11. Mukesh, K.; Mohanty, S.; Nayak, S. K.; Rahail Parvaiz, M. *Bioresour. Technol.* **2010**, *101*, 8406.
12. Run, M. T.; Wang, Y. J.; Yao, C. G.; Gao, J. G. *Thermochim. Acta* **2006**, *447*, 13.
13. Cao, X.; Mohamed, A.; Gordon, S. H.; Willett, J. L. *Thermochim. Acta* **2003**, *406*, 115.
14. Yew, G. H.; Mohd Yusof, A. M.; Mohd Ishak, Z. A.; Ishiaku, U. S. *Polym. Degrad. Stab.* **2005**, *90*, 488.
15. Chanakorn, Y.; Rangrong, Y. *Carbohydr. Polym.* **2011**, *83*, 22.
16. Avrami, M. *J. Chem. Phys.* **1939**, *7*, 1103.
17. Avrami, M. *J. Chem. Phys.* **1940**, *8*, 212.
18. Avrami. M. *J. Chem. Phys.* **1941**, *9*, 177.
19. Jeziorny, A. *Polym.* **1978**, *19*, 1142.
20. Ozawa, T. *Polym.* **1971**, *12*, 150.
21. Liu, T. X.; Mo, Z. S.; Wang, S.; Zhang, H. F. *Polym. Eng. Sci.* **1997**, *37*, 568.
22. Ren, M. Q.; Zhang, Z. Y.; Mo, Z. S.; Zhang, H. F. *Chin. Polym. Bull.* **2003**, *3*, 15.